Numerical Analysis of Electromagnetic Fields

Javier Bilbao, Eugenio Bravo, Olatz Garcia, Carolina Rebollar, and Concepcion Varela

Abstract Classically, the solution to contour problems in electromagnetism was based on analytical techniques, looking for closed solutions. The solution, whether computational or analytical, of electromagnetic problems is extremely important for analyzing the interactions of wave emitting and receiving devices among themselves and with their environment, including both inanimate dispersing objects and living beings. There are many applications in various areas: radio frequency antennas, radar, optics, wireless communications, imaging in bioengineering, nanotechnology and metamaterials, electrical substations, etc. Such analytical or computational solutions are particularly useful to increase productivity in all these well-established areas, to provide procedures to improve existing designs before actual implementations and to facilitate the design of new processes and devices. Typically, electromagnetism problems can be formulated using Maxwell equations. However, the Maxwell equations only admit an analytical solution for some dispersing or emitting objects with canonical geometric shapes, such as the sphere, the infinite plane, elemental antennas, etc. Numerical methods broaden the spectrum of known solutions which, while to be considered approximate, in many cases can be selected to what level of precision the calculated results describe the physical reality being analyzed. In recent decades,

J. Bilbao (✉) · E. Bravo · O. Garcia · C. Rebollar · C. Varela
Applied Mathematics Department, University of the Basque Country, Bilbao, Spain
e-mail: javier.bilbao@ehu.eus

E. Bravo
e-mail: eugenio.bravo@ehu.eus

O. Garcia
e-mail: olatz.garcia@ehu.eus

C. Rebollar
e-mail: carolina.rebollar@ehu.eus

C. Varela
e-mail: concepcion.varela@ehu.eus

N. Mahdavi Tabatabaei and N. Bizon (eds.), *Numerical Methods for Energy Applications*, Power Systems,
https://doi.org/10.1007/978-3-030-62191-9_19

driven by the availability of increasingly powerful computers, the area of computational electromagnetics (CEM) has experienced a remarkable increment as an area of research. Mathematical formulations of physical electromagnetic problems produce systems of equations that can now be solved numerically by computers. Thanks to advances in computational technology and increasingly sophisticated mathematical algorithms of electromagnetic modeling, it is a reality to simulate radiation or scattering problems containing arbitrary and complex structures for which there is no analytical solution to the Maxwell equations. There are various methods of computational electromagnetism and various classifications. Depending on the geometric model used by their formulations to characterize the dispersers, they can be classified into three types: ray tracing, surface discretizations, and volume discretizations. Depending on the precision achieved in the results and the field of application, they are classified into full-wave and asymptotic methods, also called low and high-frequency methods. Methods based on volumetric discretizations, such as finite-difference time-domain (FDTD) and frequency domain finite-element method (FEM), have the advantages that they allow for easy modeling of non-homogeneous media, and their associated 3D mathematical formulations are relatively simple. However, they suffer from the fact that the resulting system of linear equations has a number of unknowns proportional to the simulated volume, so the computational demand grows very rapidly as the electrical dimensions considered in the simulation increase. The methods based on discretizations of surfaces present characteristics that make them computationally more efficient than the volumetric ones. The formulations used in surface methods are based on surface integral equations (SIE) which, unlike volumetric formulations, are mathematically more difficult to implement in a computational code, partly due to the various types of singularities of the Green function. Another disadvantage of this type of methods is the impossibility of simulating general non-homogeneous means, although they have the great advantage that they only require discretizing the interfaces, that is to say, the two-dimensional surfaces that delimit the dispersing objects. Among the surface methods, the method-of-moments (MoM) and its computational optimizations stand out, in exchange for introducing a controllable numerical error on the results of the pure MoM, known as fast multipole method (FMM) and multilevel fast multipole algorithm (MLFMA). The physical optics (PO) is also considered as a surface method based on SIEs since it is based on surface discretizations, although using approximations valid only for electrically large objects. The PO supports a correction method to include diffraction, called physical theory of diffraction (PTD), although this correction is only applicable to perfect electric conductors (PEC). In this chapter, we will analyze some of the numerical methods used in electromagnetism.

Keywords Numerical analysis · Electromagnetic fields · Electromagnetism · Computational electromagnetics · Surface integral equations

Abbreviation/Acronyms

CEM	Computational electro magnetics
CFIE	Combined field integral equation
EFIE	Electric field integral equation
FDTD	Finite-difference time-domain
FE	Finite elements
FEM	Finite-element method
FMM	Fast multipole method
GMRES	Generalized minimal residual algorithm
GTD	Geometrical theory of diffraction
HF	High frequency
MECA	Modified equivalent current approximation
MFIE	Magnetic field integral equation
MLFMA	Multi level fast multipole algorithm
MoM	Method of moments
PEC	Perfect electric conductors
PO	Physical optics
PTD	Physical theory of diffraction
RWG	Rao Wilton Glisson
SIE	Surface integral equations
TE	Transverse-electric wave
TM	Transverse-magnetic wave
ε	Permittivity
σ	Conductivity
μ	Permeability
$\vec{E}$	Electric field
$\vec{H}$	Magnetic field
$\vec{J}$	Electric surface current
$\vec{M}$	Magnetic surface current
η	Impedance
L, K	Integral-differential operators
$G(\vec{r}, \vec{r}')$	Green scalar function

1 Introduction

Electromagnetic problems have a multitude of applications in our lives, in industry and particularly in engineering and they can be very different in nature. This wide range of possibilities in which to apply computational electromagnetics (CEM) and the great variety of types of problems that we can find have led scientists to create a large number of different algorithms to deal with this type of problems. However, nowadays, there is no algorithm that stands out from the rest for any situation and

problem that we are going to face. In other words, there are algorithms that are more suitable for one type of problem or conditioning and others are more suitable for another type [1–3].

The classification of these algorithms is usually done into the low frequency algorithms (or accurate algorithms) and high frequency algorithms (or approximate algorithms). Often, electromagnetic problems are also classified on the basis of the working domain: time domain or frequency domain.

Briefly, the main or most used algorithms to solve electromagnetic problems are the following [4], remembering that they are not the only ones and that they can exist, and exist, other algorithms that for certain particular problems can have an advantage of calculation on the ones mentioned here.

1.1 Low Frequency Methods

Some algorithms solve Maxwell's equations without hidden approximations and are generally applied to small electrical problems due to calculation times and system memory limitations: these algorithms are the low frequency methods. Although computers are becoming increasingly powerful and solving more and more problems, it is likely that this concept of limitation, related to the computers, can become obsolete in the medium future.

Within this type of methods, we will cite the three most used, without the order in which they appear presupposes their better or worse applicability.

1.1.1 The Finite Difference Time Domain Method

The Finite Difference Time Domain method (FDTD) uses the finite difference method in order to solve Maxwell's equations in the time domain. The implementation of the FDTD method is generally quite simple [5–8]: a solution domain is usually subdivided in small rectangular or curvilinear elements, with a "jump" in the time used to calculate the electric and magnetic fields.

FDTD works normally very well in the analysis of non-homogeneous and nonlinear media, but it requires very high quantity of dedicated memory in the computer. It is due to the discretization process of the solution of the entire domain. Usually, it is not recommended for dispersion or scattering problems. FDTD is used in waveguide packaging techniques and issues, as well as in wave propagation studies.

1.1.2 Finite Element Method

The Finite Element Method (FEM) is a method used to solve the problems of electromagnetic, with boundary values, in the frequency domain [9–12]. As FDTD method, it tries to solve Maxwell's equations in a differential way.

Although the name of the FEM has been established in the last decades of the last century, the concept has been used for several centuries. The use of temporal and spatial discretizing methods, and also numerical approximation procedures, to obtain solutions to engineering or physical problems has been known since ancient times. The concept of "finite elements" is based on this idea.

The development of finite elements as they are known today has been linked to structural calculation primarily in the aerospace field. In the 1940s, Courant [13] proposed the use of polynomial functions for the formulation of elastic problems in triangular sub-regions, as a special method of the Rayleigh-Ritz variational method to approximate solutions. It was Turner, Clough, Martin and Topp [14] who presented FEM in the form accepted today. In their work, they introduced the implementation of simple finite elements (bars and triangular plates with loads in their plane) to the analysis of aeronautical structures [15], using the concepts of discretization and functions of form.

The books by Przemieniecki [16] and Zienkiewicz and Holister [17] present the MEF in its application to structural analysis. The book by Zienkiewicz and Cheung [18] or Zienkiewicz and Taylor [19] presents a broad interpretation of FEM and its application to any field problem. It demonstrates that FE equations can be obtained using a residual weight approximation method, such as the Galerkin method or the least squares method.

It is considered as a frequency domain algorithm.

1.1.3 Method of Moments

The publication in 1968 of the work "Field Computation by Moment Methods" [20], by Harrington, allowed the systematic formulation of the existing numerical methods by means of a very general concept denoted by the Method of Moments. The method of moments is one of the most widely used numerical techniques today to determine the fields emitted or received by radiant structures.

The method of moments allows the solution of the problem of Poisson in its integral version and, in particular, to find the distribution of load on the surface of a system of conductors, known the potential to which each one of them is found. From the load distribution is obtained directly, the field and potential at any point in space.

The Method of Moments (MoM) is a technique used in the frequency domain.

1.2 High Frequency Methods

Large electromagnetic problems have set out long before the existence of computers and also some one or two decades ago, when these machines currently could not solve them. Common examples of larger problems are the prediction of the radar cross section and the calculation of the radiation pattern of an antenna when mounted on a large structure (typical use for telephony). Many approximations have been made to

the radiation and scattering equations to make these problems manageable. Most of these treat the fields at the asymptotic or high frequency (HF) boundary and employ ray optics and edge diffraction. When the problem is very large from the electrical point of view, many asymptotic methods produce results that are sufficiently accurate by themselves or can be used as a "first or previous step" before applying a more precise but computationally demanding method.

1.2.1 Theory of Geometric Diffraction and Physical Theory of Diffraction

One of the first methods for the calculation of electromagnetic diffraction was the Geometrical Theory of Diffraction (GTD) [21, 22] introduced by Keller. This method is also based on ray tracing, such as geometrical optics, but introduces diffracted rays at the edges.

When a ray hits a conductive wedge, a diffraction is observed forming a reflection angle with the same edge as the incidence. In this case, unlike what happens in flat surfaces where there is only one direction of reflection, infinite directions are observed that form with the edge an angle equal to the angle of incidence.

These directions form the so-called Keller cone [23].

The physical theory of diffraction (PTD) [24, 25], developed in parallel with Keller's theory, obtains equivalent results avoiding some problems. The result of PTD is finite and contains only the diffraction of the edge, so the fields reflected in the superficies, calculated for example by the approximation of Physical Optics (PO), must be added to it [26]. The physical theory of diffraction (PTD) is a means of complementing the PO solution by adding the effects of non-uniform currents at the diffraction edges of an object [27, 28]. PTD is commonly used in high-frequency radar cross section and scatter analysis [29].

1.2.2 Physical Optics

The method of Physical Optics (PO) consists in the fact that the currents induced on the parts of the object not illuminated, for example by a radar, are very small compared with those produced in the illuminated areas [30, 31]. In fact, the approximation made by this method consists in annulling them. For the other surfaces, the calculation will be made by obtaining the equivalent currents that would exist in a tangent infinite plane at each point of the surface.

1.2.3 Shooting and Bouncing Beams

The ray tracing is a method similar to the previous one that also takes into account the possible multiple reflections of the field reflected by the object, but its complexity is greater [32, 33].

The first reflection of the form commented in the PO method is obtained, later it is calculated if the direction of the reflection returns to intersect with some surface of the object. If so, the diffracted field that produces this new reflection is recalculated.

The calculation ends when there are no more reflections accumulating the value of all reflections. To carry it out, a large number of rays are released. These are reflected in the object according to geometric optics (Snell Law). Finally, the contributions of the rays that return to the initial position are added [34, 35].

2 Surface Integral Equations

We have focused on computational electromagnetics (CEM) based on surface integral equations (SIEs) because it provides great versatility when analyzing homogeneous and isotropic objects that occupy electrically large volumes [36]. In addition, these methods have been developed mainly since 1990.

The present chapter deals with different computational methods based on SIEs applicable to homogeneous and isotropic general media, i.e. not limited only to perfect electrical conductors (PEC) as is the case in an important part of the previous literature on EMF. Physical optics (PO) belongs to the so-called high frequency methods and allows fast predictions with a limited level of accuracy proportional to the electrical size of the objects. On the contrary, the so-called full wave methods such as the method-of-moments (MoM) allow very precise predictions of dispersed field, but their computational cost makes their application in volumes whose electrical sizes extend several wavelengths totally unfeasible. Among the techniques for accelerating MoM, the fast multipole method (FMM) [37] and its multilevel extension, based on a hierarchical multilevel partition of geometries, known as MLFMA (multilevel fast multipole algorithm) [38], stand out. In this chapter we have opted for the development of both full wave techniques (MoM, FMM, MLFMA) and high frequency (PO for penetrable media). Even hybridization between full wave and high frequency techniques could be implemented in other fields, such as radiation [39] and wave propagation [40].

This fully realistic approach, not limited to a few CEM techniques, is justified by the fact that many real problems are not fully addressable—not even using current supercomputers—but by high-frequency techniques, or by hybridizations where these operate.

3 Method of Moments

The Method of Moments (MoM) is a full wave method, introduced in CEM by R. F. Harrington in 1967. His book, currently re-published by the IEEE [20], remains a fundamental reference. The complexity of this method is of the order O(N2) in

memory and O(N3) in time in case of using to solve the system of resulting equations a direct method such as LU decomposition.

We remember that the order of a method is given by the number p which means the number of terms used in the weighted average used in that method.

Formally, the definition of the order of a method can be enunciated as follows:

Let's be p ≥ 0. It is said that a method is of order ≥p if for all sufficiently regular solution of a problem of initial values, we have

$$\max_{0 \le n \le N-1} |\sigma_n| \le C\, h^p$$

for some constant C (where C can depend on the solution x). Note that if a method has order $\geq p$ with $p > 0$, then it is consistent.

This last complexity can easily be reduced to O(N2) by replacing the direct method with an iterative method, according to Kim et al. [41], as the Generalized Minimal Residual algorithm, GMRES method [42].

MoM is a numerical method that allows solving a discretization of a surface integral equation (SIE). As a previous step to explain MoM's own discretization, we will briefly introduce the concept of SIE for a single dispersing object.

3.1 Using Surface Integral Equations for MoM

Let's be a penetrable homogeneous dispersant surrounded by an unlimited homogeneous medium. Let us denote by R_1 the region corresponding to the unlimited medium from which the incident wave proceeds. Next, we will denote by R_2 the limited region related to the dispersing object. From now on, we will associate a subscript $i = 1$ for all the quantities related to R_1 and another subscript $i = 2$ for the amounts of R_2. Each medium, for $i = 1, 2$, is characterized by its constitutive parameters, that we can resume as the following: the complex permittivity $\varepsilon_i = \varepsilon_{r,i} \cdot \varepsilon_0$ (which includes the effects of conductivity σ_i) and the complex permeability $\mu_i = \mu_{r,i} \cdot \mu_0$. Respectively, $\varepsilon_{r,i} \in \mathbb{C}$ and $\mu_{r,i} \in \mathbb{C}$ are the complex relative permittivity and the complex relative permeability of the medium in the region R_1. ε_0 and μ_0 are the constitutive parameters of the vacuum. We assume a harmonic time dependence e^{jwt} that we will omit in the use of the SIE. The process starts with an incident field ($\vec{E}_{inc}$, $\vec{H}_{inc}$), and we want to calculate a scattered field ($\vec{E}_{1,scatt}$, $\vec{H}_{1,scatt}$) for the region R_1 external to the disperser, and another scattered field ($\vec{E}_{2,scatt}$, $\vec{H}_{2,scatt}$) for the internal region R_2.

Applying the first principle of equivalence, or Love's equivalence principle (according to Medgyesi-Mitschang et al. [43]), it is possible to formulate an equivalent problem in R_1, where we will have $\vec{E}_{2,scatt} = 0$ and $\vec{H}_{2,scatt} = 0$ and it is necessary to impose electric surface currents $\vec{J}_1 = \hat{n}_1 \times \vec{H}_{1,scatt}\Big|_S$ and magnetic surface currents $\vec{M}_1 = -\hat{n}_1 \times \vec{E}_{1,scatt}\Big|_S$ on the surface S of the dispersant. This is

an equivalent problem, valid only for region R_1. In the same way, it is possible to set out an equivalent problem for R_2.

In order to deduce the generic form of an SIE, we start from the Maxwell equations for $\nabla \times \vec{E}_{1,scatt}$ and for $\nabla \times \vec{H}_{1,scatt}$, and we apply again the nabla operator in order to get two new equations of the following form: $\nabla \times \nabla \times \vec{E}_{1,scatt}$, and $\nabla \times \nabla \times \vec{H}_{1,scatt}$. Finally, we use mathematical tools. First, the vector Green theorem in these two equations on the surface S of the disperser (Poggio and Miller developed this vector theorem in a rigorous description [44]). Second, together with the previous theorem, these following four equals (two equals for fields and other two equals for currents), deduced, on the one hand, with the currents of the Love principle and, on the other hand, imposing tangential contour conditions:

$$\begin{aligned} \hat{n}_1 \times (\vec{E}_{1,scatt} - \vec{E}_{2,scatt})\Big|_S = 0 \quad &\Rightarrow \quad \underbrace{-\hat{n}_1 \times \vec{E}_{1,scatt}\Big|_S}_{\vec{M}_1} = \underbrace{\hat{n}_2 \times \vec{E}_{2,scatt}\Big|_S}_{-\vec{M}_2} \\ \hat{n}_1 \times (\vec{H}_{1,scatt} - \vec{H}_{2,scatt})\Big|_S = 0 \quad &\Rightarrow \quad \underbrace{\hat{n}_1 \times \vec{H}_{1,scatt}\Big|_S}_{\vec{J}_1} = \underbrace{-\hat{n}_2 \times \vec{H}_{2,scatt}\Big|_S}_{-\vec{J}_2} \end{aligned} \tag{1}$$

If the reader wants to deepen in the mathematical development of the previous procedure, he or she can find more information in the references of Medgyesi-Mitschang [43] and Ylä-Oijala et al. [45].

This procedure produces a tangential integral equation for the electric field and for each medium (T-EFIE, tangential electric field integral equation) and, by applying a cross product by the normal towards R_1, a normal integral equation for the electric field and for each medium (N-EFIE, normal electric field integral equation). Similarly, we can obtain the T-MFIE and the N-MFIE for the magnetic field. The eight tangential (T) and normal (N) equations of EFIE and MFIE for each medium depend on the surface currents, normal currents and the incident field, and are summarized as the following:

T-EFIE$_1$, medium 1:

T-EFIE$_2$, medium 2:

$$\vec{E}^{inc}(\vec{r})\Big|_{\tan} = L_1 \cdot \vec{J}(\vec{r})\Big|_{\tan} - K_1 \cdot \vec{M}(\vec{r})\Big|_{\tan} - \frac{1}{2}\vec{M}(\vec{r}) \times \hat{n}(\vec{r}) \tag{2}$$

$$\vec{0} = L_2 \cdot \vec{J}(\vec{r})\Big|_{\tan} - K_2 \cdot \vec{M}(\vec{r})\Big|_{\tan} + \frac{1}{2}\vec{M}(\vec{r}) \times \hat{n}(\vec{r}) \tag{3}$$

T-MFIE$_1$, medium 1:

T-MFIE$_2$, medium 2:

$$\vec{H}^{inc}(\vec{r})\Big|_{\tan} = K_1 \cdot \vec{J}(\vec{r})\Big|_{\tan} + \frac{1}{\eta_1^2} L_1 \cdot \vec{M}(\vec{r})\Big|_{\tan} + \frac{1}{2}\vec{J}(\vec{r}) \times \hat{n}(\vec{r}) \tag{4}$$

$$\vec{0} = K_2 \cdot \vec{J}(\vec{r})\Big|_{\tan} + \frac{1}{\eta_2^2} K_2 \cdot \vec{M}(\vec{r})\Big|_{\tan} - \frac{1}{2}\vec{J}(\vec{r}) \times \hat{n}(\vec{r}) \tag{5}$$

N-EFIE$_1$, medium 1:
N-EFIE$_2$, medium 2:

$$\hat{n}(\vec{r}) \times \vec{E}^{inc}(\vec{r}) = \hat{n}(\vec{r}) \times \left[L_1 \cdot \vec{J}(\vec{r}) - K_1 \cdot \vec{M}(\vec{r}) \right] - \frac{1}{2}\vec{M}(\vec{r}) \tag{6}$$

$$\vec{0} = \hat{n}(\vec{r}) \times \left[L_2 \cdot \vec{J}(\vec{r}) - K_2 \cdot \vec{M}(\vec{r}) \right] + \frac{1}{2}\vec{M}(\vec{r}) \tag{7}$$

N-MFIE$_1$, medium 1:
N-MFIE$_2$, medium 2:

$$\hat{n}(\vec{r}) \times \vec{H}^{inc}(\vec{r}) = \hat{n}(\vec{r}) \times \left[K_1 \cdot \vec{J}(\vec{r}) + \frac{1}{\eta_1^2} L_1 \cdot \vec{M}(\vec{r}) \right] + \frac{1}{2}\vec{J}(\vec{r}) \tag{8}$$

$$\vec{0} = \hat{n}(\vec{r}) \times \left[K_2 \cdot \vec{J}(\vec{r}) + \frac{1}{\eta_2^2} L_2 \cdot \vec{M}(\vec{r}) \right] - \frac{1}{2}\vec{J}(\vec{r}) \tag{9}$$

In these eight equations, $\vec{J}(\vec{r}) \equiv \vec{J}_1$ and $\vec{M}(\vec{r}) \equiv \vec{M}_1$ denote the surface equivalent currents for region R_1, a priori unknown. $\vec{J}(\vec{r})$ and $\vec{M}(\vec{r})$ are vector functions of an arbitrary point $\vec{r}$ on the surface of the dispersant. The vector $\hat{n}(\vec{r}) \equiv \hat{n}_1$ corresponds to the normal to the surface pointing to the outer region R_1. Moreover, $\eta_i = \left(\mu_i / \varepsilon_i\right)^{1/2}$ is the impedance intrinsic of the medium in R_i. The integral-differential operators L_i and K_i in these equations are defined as:

$$L_i \cdot \vec{X}(\vec{r}) = \iint_S \left[jw\mu_i \cdot \vec{X}(\vec{r}') + \frac{j}{w\varepsilon_i} \nabla \left(\nabla' \cdot \vec{X}(\vec{r}') \right) \right] \cdot G_i(\vec{r}, \vec{r}') \cdot dS'$$

$$K_i \cdot \vec{X}(\vec{r}) = P.V. \iint_S \vec{X}(\vec{r}') \times \nabla G_i(\vec{r}, \vec{r}') \cdot dS' \tag{10}$$

The *P.V.* notation is used in the definition of the K_i operator to indicate that the integration is taken as a Cauchy principal value integral (that is, when we have an improper integral, normally, a contour integral of a complex-valued function). The integration surface S alludes to the separation interface between R_1 and R_2. The term in $G_i(\vec{r}, \vec{r}')$ in the Eq. (10) is the Green scalar function for the region R_i, defined as:

$$G_i(\vec{r}, \vec{r}') = \frac{e^{(-jk_i|\vec{r}-\vec{r}'|)}}{4\pi|\vec{r} - \vec{r}'|} \tag{11}$$

In the last two equations, (10) and (11), the vector $\vec{r}'$ refers to a source point and $\vec{r}$ denotes an observation point. In addition, $k_i = w(\varepsilon_i \mu_i)^{1/2}$ is the wave number in R_i.

A generic SIE formulation can be established by combining different EFIEs and MFIEs in (2)–(9).

Table 1 Parameters to obtain the SIE formulations

SIE	a_i for $i = 1, 2$	b_i for $i = 1, 2$	c_i for $i = 1, 2$	d_i for $i = 1, 2$
PMCHWT	η_i	0	0	$1/\eta_i$
JMCFIE	1	1	1	1
CTF	1	0	0	1
CNF	0	1	1	0
MNMF	0	$\mu_i/(\mu_1 + \mu_2)$	$\varepsilon_i/(\varepsilon_1 + \varepsilon_2)$	0

We perform a general combination of these eight equations using the same sign criteria as Ergül in [46]:

$$\begin{aligned} &\frac{a_1}{\eta_1}(T - EFIE_1) + \frac{a_2}{\eta_2}(T - EFIE_2) + \\ &\quad + b_1(N - MFIE_1) - b_2(N - MFIE_2) = \vec{0} \\ &\quad - c_1(N - EFIE_1) + c_2(N - EFIE_2) + \\ &\quad + d_1\eta_1(T - MFIE_1) + d_2\eta_2(T - MFIE_2) = \vec{0} \end{aligned} \tag{12}$$

There are infinite values that can be assigned to the complex scalar parameters $a_i, b_i, c_i, d_i \in \mathbb{C}$ for $i = 1, 2$ in order to obtain valid and stable formulations. The parameters in (12) that allow to obtain some types of SIEs can be found in Table 1.

The SIE formulations in the table are well known and well reported for the case of dispersers isolated in free space. These formulations are known as Poggio-Miller-Chang-Harrington-Wu-Tsai (called by the acronym PMCHWT) [44, 47–49], combined tangential formulation (CTF) [42, 46], combined normal formulation (CNF) [45, 49], modified normal Müller formulation (MNMF) [45], and electric and magnetic current combined-field integral equation (JMCFIE) [50–54]. Other references incorporating other known stable formulations are [55, 56].

3.2 Discretization of SIE Formulations

To resolve such a SIE formulation of the form (12), the current densities $\vec{J}(\vec{r})$ and $\vec{M}(\vec{r})$, in our case unknown variables, are approximated in terms of linear combinations of known vector base functions $\vec{f}_n$, with $n = 1, 2, \ldots, N$, such as

$$\vec{J}(\vec{r}) = \sum_{n=1}^{N} J_n \cdot \vec{f}_n \,, \quad \vec{M}(\vec{r}) = \sum_{n=1}^{N} M_n \cdot \vec{f}_n \tag{13}$$

where J_n and M_n, with $n = 1, 2, \ldots, N$, are the unknown complex coefficients in the expansions of the Eq. (13). These coefficients are the unknowns determined in MoM

by solving a system of linear equations. Usually, in MoM we choose some functions $\vec{f}_n$, with $n = 1, 2, \ldots, N$, known as RWG bases (Rao-Wilton-Glisson) [57, 58], due basically to their simplicity to implement them in code.

From this point forward, we will always use the base functions of type RWG to represent $\vec{f}_n(\vec{r}') \equiv \vec{f}_n$. Each RWG base is associated with the side $n = 1, 2, 3$ of a triangle and is defined for the two triangles of the discretization that share that side. One of the triangles will be assigned with a " + " label and a "−"label will be assigned to the other side/triangle. These RWG functions fulfill the following:

$$\vec{f}_n(\vec{r}') = \frac{\vec{\rho}'^{\pm} l_n}{2A_n^{\pm}} \text{ and } \nabla' \cdot \vec{f}_n(\vec{r}') = \pm \frac{l_n}{A_n^{\pm}} \tag{14}$$

where the value A_n^+ (and/or A_n^-) denotes the area of the triangle + (or −), and l_n is the length of the side. In addition, $\vec{\rho}'^{+} = \vec{r}' - \vec{p}^{+}$ ($\vec{\rho}'^{-} = \vec{p}^{-} - \vec{r}'$) represents the vector that joins the node $\vec{p}^{+}$ ($\vec{p}^{-}$) opposite to the considered side of the triangle up to (from) the source point $\vec{r}'$ on the triangle + (or −).

Applying the so-called Galerkin procedure, each side of the triangle is assigned a weighting function (also called a test function) denoted as $\vec{f}_m(\vec{r}) \equiv \vec{f}_m$, which has the same vector expression as the corresponding base function $\vec{f}_n(\vec{r}') \equiv \vec{f}_n$ assigned to the same side. For simplicity, the weighting operation, or test operation, using a function $\vec{f}_m(\vec{r}) \equiv \vec{f}_m$ to weight a generic vector $\vec{v}_n(\vec{r})$, we will denote as:

$$\left\langle \vec{f}_m, \vec{v}_n \right\rangle = \iint_{S_m} \vec{f}_m(\vec{r}) \cdot \vec{v}_n(\vec{r}') \cdot dS \tag{15}$$

where the dot operator within the integral represents an inner product, and S_m is the area of integration over which $\vec{f}_m$ is defined.

Substituting (14) in (13) and weighting with functions $\vec{f}_m$, with $m = 1, \ldots, N$, finally we find a linear equation system $\bar{\bar{Z}} \cdot \vec{I} = \vec{V}$ of dimensions 2 N *x* 2 N:

$$\bar{\bar{Z}} \cdot \vec{I} = \vec{V}\ , \quad \bar{\bar{Z}} = \begin{bmatrix} \bar{\bar{Z}}^{J,(T-EFIE,N-MFIE)} & \bar{\bar{Z}}^{M,(T-EFIE,N-MFIE)} \\ \bar{\bar{Z}}^{J,(T-MFIE,N-EFIE)} & \bar{\bar{Z}}^{M,(T-MFIE,N-EFIE)} \end{bmatrix} \tag{16}$$

The inputs for the five sub-matrixes N × N are given by the following expressions for $m = 1, \ldots, N$ and $n = 1, \ldots, N$:

$$\begin{aligned} \bar{\bar{Z}}_{m,n}^{J,(T-EFIE,N-MFIE)} = & \left\langle \vec{f}_m, \left(\frac{a_1}{\eta_1} L_1 + \frac{a_2}{\eta_2} L_2 \right) \vec{f}_n \right\rangle + \\ & + \left\langle \vec{f}_m, \hat{n}_m \times (b_1 K_1 - b_2 K_2) \vec{f}_n \right\rangle + \\ & + \frac{b_1 + b_2}{2} \left\langle \vec{f}_m, \vec{f}_n \right\rangle \end{aligned} \tag{17}$$

$$\begin{aligned}\bar{\bar{Z}}_{m,n}^{M,(T-EFIE,N-MFIE)} &= -\left\langle \vec{f}_m, \left(\frac{a_1}{\eta_1}K_1 + \frac{a_2}{\eta_2}K_2\right)\vec{f}_n \right\rangle + \\ &+ \frac{1}{2}\left(\frac{a_1}{\eta_1} - \frac{a_2}{\eta_2}\right)\left\langle \vec{f}_m, \hat{n}_m \times \vec{f}_n \right\rangle + \\ &+ \left\langle \vec{f}_m, \hat{n}_m \times \left(\frac{b_1}{\eta_1^2}L_1 - \frac{b_2}{\eta_2^2}L_2\right)\vec{f}_n \right\rangle \end{aligned} \tag{18}$$

$$\begin{aligned}\bar{\bar{Z}}_{m,n}^{J,(T-MFIE,N-EFIE)} &= \left\langle \vec{f}_m, \hat{n}_m \times (-c_1 L_1 + c_2 L_2)\vec{f}_n \right\rangle + \\ &+ \left\langle \vec{f}_m, (d_1\eta_1 K_1 + d_2\eta_2 K_2)\vec{f}_n \right\rangle - \\ &- \frac{d_1\eta_1 - d_2\eta_2}{2}\left\langle \vec{f}_m, \hat{n}_m \times \vec{f}_n \right\rangle \end{aligned} \tag{19}$$

$$\begin{aligned}\bar{\bar{Z}}_{m,n}^{M,(T-MFIE,N-EFIE)} &= \left\langle \vec{f}_m, \hat{n}_m \times (c_1 K_1 - c_2 K_2)\vec{f}_n \right\rangle + \frac{c_1 + c_2}{2}\left\langle \vec{f}_m, \vec{f}_n \right\rangle + \\ &+ \left\langle \vec{f}_m, \left(\frac{d_1}{\eta_1}L_1 + \frac{d_2}{\eta_2}L_2\right)\vec{f}_n \right\rangle \end{aligned} \tag{20}$$

We can write the $\vec{I}$ vector, which contains the unknowns (coefficients of the RWG bases) of the linear system, as the following:

$$\vec{I} = (J_1, J_2, \ldots, J_N, M_1, M_2, \ldots, M_N)^T \tag{21}$$

And the $\vec{V}$ excitation vector of the lineal system is:

$$\begin{aligned}\vec{V} &= \begin{bmatrix} \vec{V}^{(T-EFIE,N-MFIE)} \\ \vec{V}^{(T-MFIE,N-EFIE)} \end{bmatrix} = \\ &= (V_1^{(T-EFIE,N-MFIE)}, \ldots, V_N^{(T-EFIE,N-MFIE)}, V_1^{(T-MFIE,N-EFIE)}, \ldots, V_N^{(T-MFIE,N-EFIE)})^T \end{aligned} \tag{22}$$

where the coefficients are the following;

$$\begin{aligned} V_m^{(T-EFIE,N-MFIE)} &= \frac{a_1}{\eta_1}\left\langle \vec{f}_m, \vec{E}^{inc}(\vec{r}) \right\rangle + b_1\left\langle \vec{f}_m, \hat{n}_m \times \vec{H}^{inc}(\vec{r}) \right\rangle \quad \text{para } m = 1, \ldots, N \\ V_m^{(T-MFIE,N-EFIE)} &= -c_1\left\langle \vec{f}_m, \hat{n}_m \times \vec{E}^{inc}(\vec{r}) \right\rangle + d_1\eta_1\left\langle \vec{f}_m, \vec{H}^{inc}(\vec{r}) \right\rangle \quad \text{para } m = 1, \ldots, N \end{aligned} \tag{23}$$

Once the linear system is resolved, the current densities $\vec{J}(\vec{r})$ and $\vec{M}(\vec{r})$, calculated at each point, can be determined with (14). The electric field scattered at any point in space, inside and outside the disperser, can be calculated directly with $\vec{J}(\vec{r})$ and $\vec{M}(\vec{r})$, using the following two expressions:

$$\vec{E}_{1,scatt}(\vec{r}) = -L_1\vec{J}(\vec{r}) + K_1\vec{M}(\vec{r})$$
$$\vec{E}_{2,scatt}(\vec{r}) = L_2\vec{J}(\vec{r}) - K_2\vec{M}(\vec{r}) \tag{24}$$

The above expressions for scattered field can be derived by following the theoretical development to Eq. (1), but without applying the equalities in (1) to the field vectors. It is important to note that the field equations in (24) are valid for any point of the space and they do not impose any restrictions on the size of the dispersers.

Typically, (24) is known as "near field expressions". For far-field, these expressions are also valid, but it should be much more computationally efficient to use a simplified expression.

Sometimes, the implementation of MoM in computers requires some extra procedures. For example, the integrals of the operators L_i and K_i in (10) can be calculated numerically by a rule of Gaussian quadrature consisting of seven points per triangle, as described Gibson [4]. In this same reference, some theoretical procedures to extract the singularities that occur in integrals when the source point and the observation point are close to each other, $\left|\vec{r} - \vec{r}'\right| \to 0$, can be found.

4 Physical Optics

Physical optics (PO) is a computational technique of high frequency used to calculate the electromagnetic dispersion coming from complex and electrically large PEC (perfect electric conductor) structures [59, 60]. Unlike so-called full-wave methods, for example the method of moments (MoM), the PO does not require high amounts of computational resources to solve dispersion problems with acceptable levels of precision and, above all, with a high efficiency. In this way, simulations that normally take hours with the method of moments, typically are resolved in just a few seconds or minutes with the PO.

4.1 MECA Method

The MECA (modified equivalent current approximation) method [61, 62], has extended PO to dielectric materials with losses characterized by complex effective permittivity. In MECA, the equivalent magnetic and electrical currents are calculated based on the incidence of a locally plane wave on the surface of the dispersant. The MECA equations are derived using a decomposition of the incident field into TE (transverse-electric wave) and TM (transverse-magnetic wave) components, relative to the incident direction and to the normal vectors of each triangular facet in which the surface of the dispersant is discretized. Contrary to what happens in other generalizations of the PO for dielectric media [63–65], MECA takes into account the differences between the TE and TM components, with the consequent increase

in accuracy. In addition, unlike previous approaches, the current distribution on each facet has a uniform amplitude and a distribution of phase that is linear. Therefore, the radiation integral can be resolved in an analytic way and, thus, some difficult problems for a full-wave simulation, especially at very high frequencies, are successfully modelled with MECA.

In the MECA method, the equivalent current densities, magnetic and electrical, are calculate at the barycenter of each facet using the following two equations, respectively:

$$\begin{aligned}\vec{M}_{i0} &= E^i_{TE}(1+R_{TE})(\hat{e}_{TE}\times\hat{n}_i) + E^i_{TM}\cos(\theta_{inc})(1+R_{TM})\,\hat{e}_{TE}\big|_{S_i}\\ \vec{J}_{i0} &= \frac{E^i_{TE}}{\eta_1}\cos(\theta_{inc})(1-R_{TE})\hat{e}_{TE} + \frac{E^i_{TM}}{\eta_1}(1-R_{TM})\,(\hat{n}_i\times\hat{e}_{TE})\big|_{S_i}\end{aligned} \tag{25}$$

where η_1 is the impedance in the medium of incidence, and R_{TE} (and R_{TM}) is the TE (TM) reflection coefficient. The expressions of these two coefficients can be found in work of Meana et al. [62].

As shown in Fig. 2.1, $\vec{E}^i_{TE} = E^i_{TE}\hat{e}_{TE}$ and $\vec{E}^i_{TM} = E^i_{TM}\hat{e}_{TM}$ are the TE and TM components of the incident electric field at the barycenter of the triangle S_{i}. In addition, $\hat{p}_i$ is a unit vector pointing in the direction of propagation of the incident wave, θ_{inc} is the angle of incidence, and $\hat{n}_i$ is the unit normal vector with outgoing direction of the S_{i} triangular facet. The first medium is characterized by its constitutive parameters: permittivity ε_1, permeability μ_1 and conductivity σ_1. Similarly, the second medium is characterized by ($\varepsilon_2,\ \mu_2,\ \sigma_2$). The reflection coefficients R_{TE} and R_{TM} depend on all these constitutive parameters. A reflection coefficient is defined for an incidence medium and for a dispersing medium (Fig. 1).

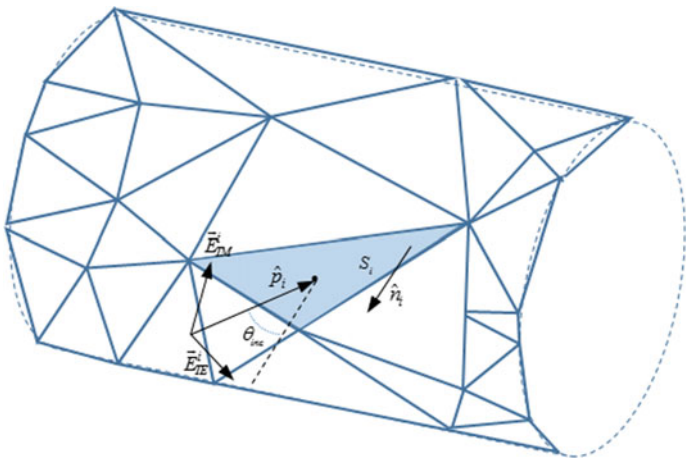

Fig. 1 Oblique incidence on a S_{i} triangular facet

The theoretical calculation of the reflection coefficients R_{TE} and R_{TM} is performed by assuming a locally specular reflection and imposing contour conditions. Ideally, the MECA method would be accurate if the dispersing object were an infinite and homogeneous semi-space. This method, therefore, presents two main sources of error for the TE polarization (analogous for TM, replacing the electric field with the magnetic one). One of the sources of error is in the lack of modeling of diffraction phenomena in the formulation. The other source of error is that multiple reflections are not considered, although this second type of error can be mitigated by iteratively applying coefficients of reflection on discontinuities.

After obtaining the current densities $\vec{M}_{i0}$ and $\vec{J}_{i0}$, an analytical solution can be derived for the radiation integral corresponding to the observation point $\vec{r}_k$, which is located in the far field of each of the triangular facets. The scattered electric field $\vec{E}_k^s$ in $\vec{r}_k$, due to the contribution of all i facets of a given mesh, can be obtained, according to Balanis [66], as:

$$\vec{E}_k^s = \frac{j}{2\lambda} \sum_i \frac{e^{-jk_1 r_{ik}}}{r_{ik}} (\vec{E}_{ik}^a - \eta_1 \vec{H}_{ik}^a \times \vec{r}_{ik}) \tag{26}$$

where λ is the wavelength in the medium of incidence, k_1 is the wave number in the medium of incidence, and $\vec{r}_{ik} = r_{ik}\hat{r}_{ik}$ is the position vector from the barycenter $\vec{r}_i$ of the ith facet to the observation point $\vec{r}_k$. The Eq. (26) is valid when $k_1|\vec{r}_k| \gg 1$. Figure 2.2 summarizes all notation for the position vectors involved in all the scatter calculations that we have used (Fig. 2).

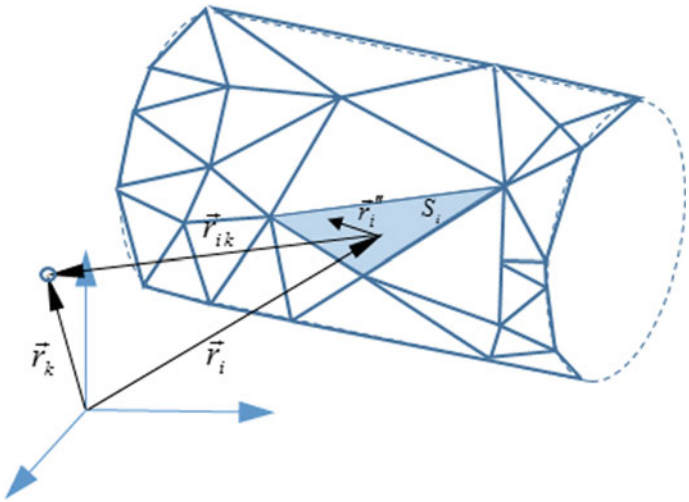

Fig. 2 S_i facet, observation point $\vec{r}_k$ and corresponding position vectors. $\vec{r}_i''$ denotes a variable vector from the barycenter $\vec{r}_i$ to any point on S_i

Assuming that currents have a constant amplitude and a phase variation that is linear and depends on the propagation direction of the incident wave, $\hat{p}_i$, the vector values $\vec{E}^a_{ik}$ and $\vec{H}^a_{ik}$ of the Eq. (26) can be calculated, according to Meana [60], as:

$$\vec{E}^a_{ik} = (\hat{r}_{ik} \times \vec{M}_{i0}) I_i(\hat{r}_{ik}) \tag{27}$$

$$\vec{H}^a_{ik} = (\hat{r}_{ik} \times \vec{J}_{i0}) I_i(\hat{r}_{ik}) \tag{28}$$

where $\vec{M}_{i0}$ and $\vec{J}_{i0}$ are the current densities given in Eqs. (25), and $I_i(\hat{r}_{ik})$ is an integral given by:

$$I_i(\hat{r}) = \iint_{S_i} e^{jk_1(\hat{r}-\hat{p}_i)\cdot\vec{r}''_i}\, dS_i \tag{29}$$

where $\vec{r}''_i$ is a variable vector from the barycenter $\vec{r}_i$ of the ith facet to the points placed on the S_i triangular surface, as it is shown in Fig. 3.

These current distributions make possible to carry out a modelling with facets bigger than those used in other high-frequency methods. This fact implies a computational cost reduction in terms of both time and memory.

The integral of Eq. (29) always admits an analytical solution, according to the procedure described by Arias-Acuña et al. [67]. The method to solve analytically is briefly summarized below.

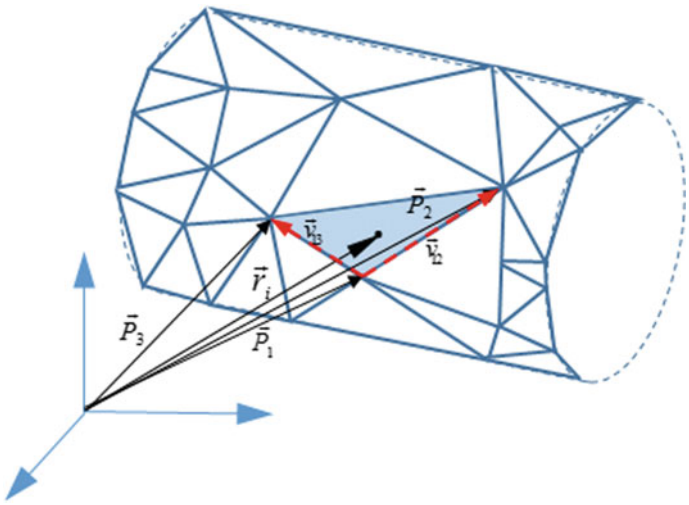

Fig. 3 Triangular facet with barycenter $\vec{r}_i$ and vertices $\vec{P}_1$, $\vec{P}_2$, and $\vec{P}_3$

First, it is considered a plane triangular facet (as shown in Fig. 3). The i triangle is defined by three points: $\vec{P}_1$, $\vec{P}_2$, and $\vec{P}_3$. And $\vec{r}_i$ is a reference point located in the barycenter ($\vec{r}_i = (\vec{P}_1 + \vec{P}_2 + \vec{P}_3)/3$).

We define $\vec{v}_{mn}$ as a vector such that $\vec{v}_{mn} = \vec{P}_n - \vec{P}_m \ , \quad m, n \in \{1, 2, 3\}$. The vector $\hat{n}$, normal to the i triangle, is defined so that $\vec{v}_{12} \times \vec{v}_{13} = 2A_i\hat{n}$, as shown in Fig. 2.3, being A_i the area of that triangle.

Finally, we use a coordinate system with two scalar variables (u, v) such that any point $\vec{r}_i''$ of the surface of the triangle can be described as:

$$\vec{r}_i'' = \vec{P}_1 - \vec{r}_i + u \cdot \vec{v}_{12} + v \cdot \vec{v}_{13} \tag{30}$$

The integral (29) is given by:

$$I_i(\hat{r}) = 2A_i e^{-j\frac{\alpha+\beta}{3}} \int_{u=0}^{u=1} \int_{v=0}^{v=1-u} e^{j(\alpha u+\beta v)} dv du \tag{31}$$

and its solution is:

$$I_i(\hat{r}) = 2A_i e^{-j\frac{\alpha+\beta}{3}} \left[\frac{\alpha e^{j\beta} - \beta e^{j\alpha} + \beta - \alpha}{\alpha\beta(\alpha - \beta)} \right] \tag{32}$$

where

$$\alpha = k_1 \vec{v}_{12}(\hat{r} - \hat{p}_i) \tag{33}$$

$$\beta = k_1 \vec{v}_{13}(\hat{r} - \hat{p}_i) \tag{34}$$

The expression (32) has the following four eigenvalues:

$$\alpha = 0, \beta \neq 0 \Rightarrow I_i(\hat{r}) = 2A_i \ e^{-j\frac{\beta}{3}} \ \frac{1 + j\beta - e^{j\beta}}{\beta^2} \tag{35}$$

$$\alpha \neq 0, \beta = 0 \Rightarrow I_i(\hat{r}) = 2A_i \ e^{-j\frac{\alpha}{3}} \ \frac{1 + j\alpha - e^{j\alpha}}{\alpha^2} \tag{36}$$

$$\alpha = \beta \neq 0 \Rightarrow I_i(\hat{r}) = 2A_i \ e^{j\frac{\alpha}{3}} \ \frac{1 - j\alpha - e^{-j\alpha}}{\alpha^2} \tag{37}$$

$$\alpha = \beta = 0 \Rightarrow I_i(\hat{r}) = A_i$$

5 Comparison Between Method of Moments and Modified Equivalent Current Approximation

In this section, we do to a graphical comparison that allows to easily show the difference between PO and MoM in terms of accuracy level. Figure 2.4 shows the monostatic radar cross section (RCS) of a sphere, defined as the following:

$$RCS_{mono} = \lim_{r\to\infty}\left(4\pi r^2\left|\vec{E}_{1,scatt}(r,\theta_{inc},\phi_{inc})\right|^2/\left|\vec{E}^{inc}\right|^2\right) \tag{38}$$

where a is the radius of the sphere and $\frac{2\pi}{\lambda}$ is the wave number in the medium of incidence. In case, $\vec{E}^{inc}$ is a uniform plane wave. Two cases are included in Fig. 4: PEC sphere and dielectric sphere with losses simulated with MECA for the parameters shown in the Table 2.

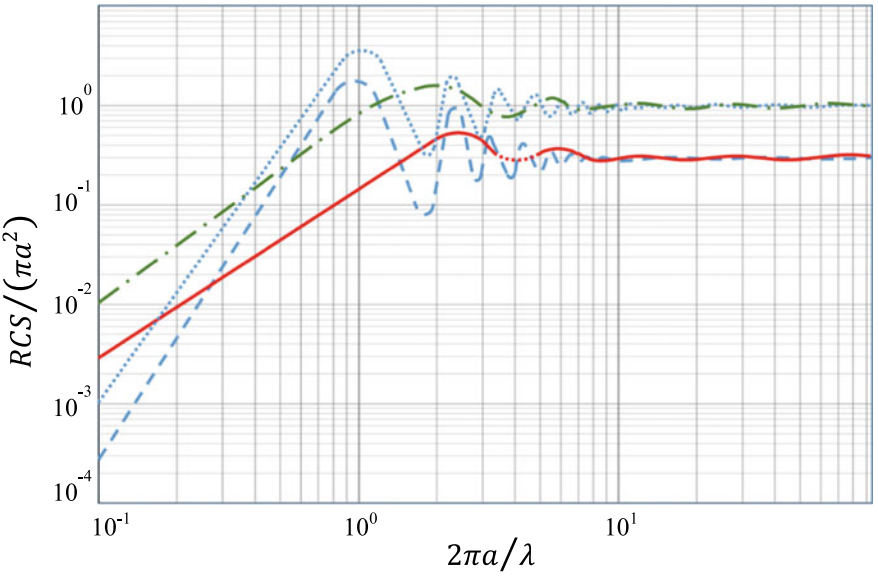

Fig. 4 Comparison between PO (MECA) and MoM solutions for scattering due to a sphere of radius a with different constitutive parameters

Table 2 Parameters used in the simulation of Fig. 4

	ε_r	μ_r	RCS
MECA	1.8	1.5	$10w\varepsilon_0$
MoM	1.8	1.5	$10w\varepsilon_0$

6 Conclusions

Techniques to solve classical electromagnetism problems have evolved over time. At first, the analysis and design of electromagnetic devices and structures was done experimentally, achieving their characterization; this result was used for the development of new technologies. Subsequently, analytical models emerged where closed form solutions are obtained, that is, solutions that model and describe the electromagnetic phenomenon through a simplified algebraic equation under ideal situations.

At present, the numerical solution is arrived at using computational algorithms, in which various numerical analysis techniques are used that describe the phenomena in time and space of electromagnetic problems that previously could not be solved analytically. In fact, many numerical analysis techniques have been developed in recent years, leading to advances in this area, referred to as computational electromagnetism (CEM). Similarly, the wide range of electromagnetic problems has led to the development of different algorithms in computational electromagnetism, each with its advantages and limitations.

Numerical solutions to three-dimensional electromagnetic dispersion problems are generally found on the formulation of surface integral equations, such as the electric field integral equations (EFIE) and the similar magnetic field integral equations (MFIE), or even the less used combined field integral equation (CFIE). The moment method (MoM) is, at present, one of the most commonly used numerical method to solve these type of equations. In the solution of this method, the induced electric current and magnetic current are unknown variables. Moreover, the surface is generally partitioned into small flat patches. In these patches, the currents are approximately calculated by some appropriate basic functions.

These patches have simple shapes to be easier implemented and for doing calculations in also easier way. The most commonly used forms for this partition or division are triangular and rectangular patches. If the size of these subdivisions (patches) is small enough, then we could approximate the induced surface currents by the triangular (or rectangular) functions of the ceiling. The application of these type of functions using the method of moment in order to solve the surface integral equations has the consequence of the evaluation of double integrals with single cores.

The Method of Moments (MoM) is a numerical technique used to convert the integral equation into a linear system, which can be solved using a computer.

The main reasons why researchers select this method are:

- It solves the Maxwell equations without implicit approximations.
- It presents greater numerical stability in the discretization of integrals versus derivatives.
- It allows to exclude the medium that is around the structure and therefore facilitates the analysis of open structures.
- It analyzes the problem in a rigorous and precise way, taking into account most of the physical phenomena that occur in the structures, so that the analysis is valid in principle for any frequency.

This method allows the systematic formulation of the problem through the discretization of the electric field integral equation (EFIE), and calculates by numerical methods the densities of unknown currents. However, it presents a disadvantage, which is given from restricting it to problems of small electrical size due to limitations in memory and time in the computational process.

References

1. Sadiku M (2018) Elements of electromagnetics, 7th edn. Oxford University Press
2. Christiansen D, Jurgen R, Fink D (1996) Electronics engineers handbook (standard handbook of electronics engineering), 4th edn. McGraw-Hill Education
3. Baro I, Bilbao J, Varela C (2007) Linear algebra (*in Basque: Aljebra lineala*). Ed. Centro de Publicaciones de la Escuela Técnica Superior de Ingenieros Industriales y de Telecomunicación de Bilbao, ISBN: 978-84-95809-31-5
4. Gibson WC (2014) The method of moments in electromagnetics, 2nd edn. Chapman & Hall/CRC
5. Taflove A, Hagness SC (2005) Computational electrodynamics: the finite-difference time-domain method, 3rd edn. Artech House
6. Kunz K, Luebbers R (1993) The finite difference time domain method for electromagnetics. CRC Press
7. Thomas JW (1995) Numerical partial differential equations: finite difference methods. Springer Verlag, Berlin, Germany
8. Kermani MH, Ramahi OM (2006) The complementary derivatives method: a second-order accurate interpolation scheme for non-uniform grid in FDTD simulation. IEEE Microw Wireless Compon Lett 16:60–62
9. Jin J (1993) The finite element method in electromagnetics. Wiley
10. Volakis JL, Chatterjee A, Kempel LC (1998) Finite element method for electromagnetics. IEEE Press
11. Bathe KJ (1995) Finite element procedures, 2nd edn. Prentice Hall
12. Polycarpou AC (2006) Introduction to the finite element method in electromagnetics. Synthesis Lect Comput Electromag 1(1):1–126
13. Courant R (1943) Variational methods for the solution of problems of equilibrium and vibrations. Bull Am Math Soc 49:1–43
14. Turner MJ, Clough RW, Martin HC, Topp LJ (1956) Stiffness and deflection analysis of complex structures. J Aeronaut Sci 23:805–824
15. Bilbao J, Bravo E, García O, Varela C, Rodríguez M, González P (2015) Blade aerodynamic design and analysis as first step to achieve the expected power performance of a small wind turbine. Int J Tech Phys Prob Eng 3(7):42–46
16. Przemieniecki JS (1968) Theory of matrix structural analysis. Mc GRaw-Hill, New York
17. Zienkiewicz OC, Holister GS (1965) Stress analysis. Wiley, London
18. Zienkiewicz OC, Cheung YK (1967) The finite element method in structural and continuum mechanics. Mc Graw-Hill, London
19. Zienkiewicz OC, Taylor RL, Zhu JZ (2005) The finite element method: its basis and fundamentals, 6th edn. Elsevier
20. Harrington RF (1993) Field computation by moment methods. IEEE Press. Series on Electromagnetic Waves, pp. 15–64
21. Keller JB (1962) Geometrical theory of diffraction. J Opt Soc Am 52:116–130
22. Kouyoumjian RG, Pathak PH (1974) A uniform geometrical theory of diffraction for and edge in a perfectly conducting surface. Proc IEEE 62:1448–1461
23. Keller J (1960) Backscattering from a finite cone. IRE Trans Antennas Propag 8(2)

24. Ufimtsev PY Method of edge waves in the physical theory of diffraction. Foreign Technology Div Wright-Patterson AFB, Ohio. Retrieved from: https://apps.dtic.mil/dtic/tr/fulltext/u2/733203.pdf
25. Ufimtsev PY (2014) Fundamentals of the physical theory of diffraction, 2nd edn. Wiley
26. Akhiyarov VV, Borzov AB, Likhoedenko KP, Karakulin YV, Seregin GM, Suchkov VB (2018) Mathematical simulation of electromagnetic scattering field from perfectly conducting object with dielectric cover on the base of physical theory of diffraction. In: CSAE '18 proceedings of the 2nd international conference on computer science and application engineering, article No. 67, Hohhot, China, October 22–24
27. Ufimtsev PY (1957) Approximate computation of the diffraction of plane electromagnetic waves at certain metal bodies (i and ii). Sov Phys Tech 27:1708–1718
28. Michaeli A (1984) Equivalent edge currents for arbitrary aspects of observation. IEEE Trans Antennas Propag 23:252–258
29. Lee H, Koh IS (2018) Consideration of diffraction effect in iterative physical optics combining physical theory of diffraction for conducting body. In: 12th European conference on antennas and propagation (EuCAP 2018)
30. Balanis CA (1989) Advanced engineering electromagnetics. Wiley
31. Al-Azzawi A (2018) Physical optics: principles and practices. CRC Press
32. Canta SM, Kipp RA, Carpenter S, Petersson LER (2018) Range-Doppler radar signature prediction of wind turbine using SBR. In: 12th European conference on antennas and propagation (EuCAP 2018)
33. Ghanmi H, Khenchaf A, Pouliguen P (2018) Radar cross section of modified target using gaussian beam methods: experimental validation. In: 2018 international conference on radar (RADAR)
34. Ling SLH, Chou R (1989) Shooting and bouncing rays: calculating the RCS of an arbitrarily shaped cavity. IEEE Trans Antennas Propag 37:194–205
35. Ling SLH, Chou R (1989) High-frequency RCS of open cavities with rectangular and circular cross sections. IEEE Trans Antennas Propag 37:648–652
36. Yilmaz AE, Jin JM, Michielssen E (2004) Time domain adaptive integral method for surface integral equations. IEEE Trans Antennas Propag 52(10)
37. Engheta N, Murphy WD, Rokhlin V, Vassiliou MS (1992) The fast multipole method (FMM) for electromagnetic scattering problems. IEEE Trans Antennas Propag 40(6)
38. Song J, Lu CC, Chew WC (1997) Multilevel fast multipole algorithm for electromagnetic scattering by large complex objects. IEEE Trans Antennas Propag 45(10)
39. Hasanov ER, Hajiyeva VM, Salimi Rikani A, Tabatabaei NM (2019) Radiation doped semiconductors with certain impurities. Int J Tech Phys Prob Eng (IJTPE) 11(2):13–17
40. Akbarli RS (201) Waves propagation in the fluid flowing in an elastic tube, considering viscoelastic friction of surrounding medium. Int J Tech Phys Propag Eng (IJTPE) 10(2):39–42
41. Kim OS, Meincke P, Breinbjerg O (2004) Method of moments solution of volume integral equations using higher-order hierarchical Legendre basis functions. Radio Sci 39:RS5003
42. Saad Y, Schultz M (1986) GMRES: a generalized minimal residual algorithm for solving non-symmetric linear systems. SIAM J Sci Stat Comput 7(15):856–869
43. Medgyesi-Mitschang LN, Putnam JM, Gedera MB (1994) Generalized method of moments for three-dimensional penetrable scatterers. J Opt Soc Am A 11(4):1383–1398
44. Poggio AJ, Miller EK (1973) Integral equation solutions of three-dimensional scattering problems. In: Mittra R (edn) Computer techniques for electromagnetics. Pergamon Press, Oxford
45. Ylä-Oijala P, Taskinen M, Järvenpää S (2005) Surface integral equation formulations for solving electromagnetic scattering problems with iterative methods. Radio Sci 40(6):RS6002
46. Ergül Ö (2009) Accurate and efficient solutions of electromagnetics problems with the multilevel fast multipole algorithm. Ph.D. dissertation, Bilkent University, Ankara, Turkey, 2009. Retrieved from: https://core.ac.uk/download/pdf/52925780.pdf
47. Chang Y, Harrington RF (1977) A surface formulation for characteristic modes of material bodies. IEEE Trans Antennas Propag 25:789–795

48. Wu TK, Tsai LL (1977) Scattering from arbitrarily-shaped lossy dielectric bodies of revolution. Radio Sci 12:709–718
49. Ergül Ö, Gürel L (2008) Novel electromagnetic surface integral equations for highly accurate computations of dielectric bodies with arbitrarily low contrasts. J Comput Phys 227(23):9898–9912
50. Ylä-Oijala P, Taskinen M (2005) Application of combined field integral equation for electromagnetic scattering by dielectric and composite objects. IEEE Trans Antennas Propag 53(3):1168–1173
51. Ylä-Oijala P (2008) Numerical analysis of combined field integral equation formulations for electromagnetic scattering by dielectric and composite objects. Prog Electromagn Res C 3:19–43
52. Cui Z, Han Y, Xu Q, Li M (2010) Parallel MoM solution of JMCFIE for scattering by 3-D electrically large dielectric objects. Prog Electromagn Res M 12:217–228
53. Taboada JM, Rivero J, Obelleiro F, Araujo MG, Landesa L (2011) Method-of-moments formulation for the analysis of plasmonic nano-optical antennas. J Opt Soc Am A 28(7):1341–1348
54. Araujo MG, Taboada JM, Rivero J, Solís DM, Obelleiro F (2012) Solution of large-scale plasmonic problems with the multilevel fast multipole algorithm. Opt Lett 37(3):416–418
55. Ergül Ö, Gürel L (2008) Stabilization of integral-equation formulations for the accurate solution of scattering problems involving low-contrast dielectric objects. Trans Antennas Propag 56(3):799–805
56. Ergül Ö, Gürel L (2009) Comparison of integral-equation formulations for the fast and accurate solution of scattering problems involving dielectric objects with the multilevel fast multipole algorithm. IEEE Trans Antennas Propag 57(1):176–187
57. Rao SM, Wilton DR, Glisson AW (1982) Electromagnetic scattering by surfaces of arbitrary shape. IEEE Trans Antennas Propag 30(3):409–418
58. Li X, Lei L, Chen Y, Jiang M, Nie Z, Hu J (2019) Efficient electromagnetic analysis for complex planar thin-layer composite objects by a hybrid method. IEEE Antennas Wireless Propag Lett 18(9)
59. Uluisik C, Cakir G, Cakir M, Sevgi L (2008) Radar cross section (RCS) modeling and simulation, part 1: a tutorial review of definitions, strategies, and canonical examples. Antennas Propag Mag IEEE 50(1):115–126
60. Martínez-Lorenzo JA, Pino AG, Vega I, Arias M, Rubiños O (2005) ICARA: induced-current analysis of reflector antennas. Antennas Propag Mag IEEE 47(2):92–100
61. Meana JG, Martínez-Lorenzo JA, Las-Heras F, Rappaport C (2009) A PO MoM comparison for electrically large dielectric geometries. In: Antennas and propagation society international symposium, 2009. APSURSI '09, IEEE. 1–5 June 2009
62. Meana JG, Martínez-Lorenzo JA, Las-Heras F, Rappaport C (2010) Wave scattering by dielectric and lossy materials using the modified equivalent current approximation (MECA). IEEE Trans Antennas Propag 58(11):3757–3761
63. Rengarajan SR, Gillespie ES (1988) Asymptotic approximations in radome analysis. IEEE Trans Antennas Propag 36(3):405–414
64. Hodges RE, Rahmat-Samii Y (1993) Evaluation of dielectric physical optics in electromagnetic scattering. In: Proceedings 1993 antennas and propagation society international symposium, USA
65. Sáez de Adana F, Gutierrez O (2010) Practical applications of asymptotic techniques in electromagnetics. Artech House, 2010
66. Balanis CA (1997) Antenna theory: analysis and design. Wiley, New York
67. Arias-Acuña M, Rubiños O, Cuiñas I, Pino AG (2000) Electromagnetic scattering of reflector antennas by fast physical optics algorithms. Recent Res Dev Magn 1:43–63